TURNOVER OF ROD PHOTORECEPTOR OUTER SEGMENTS

I. Membrane Addition and Loss in Relationship to Temperature

JOE G. HOLLYFIELD, JOSEPH C. BESHARSE, and MARY E. RAYBORN

From the Departments of Anatomy and Ophthalmology, College of Physicians and Surgeons, Columbia University, New York 10032. The present address for Dr. Hollyfield and Ms. Rayborn is the Department of Ophthalmology, Baylor College of Medicine, Houston, Texas 77030. Dr. Besharse's present address is the Department of Anatomy, Emory University, School of Medicine, Atlanta, Georgia 30322.

ABSTRACT

Membrane turnover in outer segments of *Rana pipiens* red rods (ROS) was studied in tadpoles maintained under cyclic lighting (12L:12D) at 23°, 28°, and 33°C. Large fragments (>2 μm in diameter or length) were shed from the ROS tips shortly after the onset of light. These were phagocytized by the pigment epithelium (PE) which caused an increase in the number of phagosomes >2 μm in size (large phagosomes). Large phagosomes were present in highest numbers 2–4 h after light exposure and were degraded by 8–12 h. The proportion of ROS that shed each day after the onset of the light cycle increased with increment increases in temperatures (23°C–18%, 28°C–33%, 33°C–42% per day), resulting in a reduction in the average interval of time between repeated sheddings (23°C–5.6 days, 28°C–3 days, 33°C–2.4 days) though the average numbers of disks shed from ROS at the various temperatures were not significantly different (23°C–139.5 ± 5.7, 28°C–129.4 ± 7.6, 33°C–129.9 ± 4.8 disks/shed packet). Phagosomes in the PE that were <2 μm in diameter (small phagosomes) were present in relatively constant numbers throughout the day, and their numbers increased at higher temperatures. The absence of a concomitant increase in small phagosomes as large phagosomes were degraded indicates that large phagosomes were not the major source of small phagosomes. When the PE was isolated to culture in the absence of the retina, these small phagosomes were degraded. The rate of disk addition to the ROS base was determined by autoradiography after [^{3}H]leucine injection. The number of disks added per day increased with elevations of temperature (23°C–32.4; 28°C–55.9; 33°C–65.5). The average number of disks added to the ROS between repeated sheddings (23°C–181.4; 28°C–167.7; 33°C–157.2) was greater than the number of disks shed after light exposure. Inasmuch as the ROS show no net increase in length during the tadpole stages utilized, the remaining disks must be lost at some other time. Electron microscope analysis revealed the presence of small groups of disks in curled configurations at the tips of ROS, suggesting possible stages of detachment. These irregular disk configurations were identical in size to the small phogosomes

in the PE, and they were observed at all fixation times studied throughout the day. Our data indicate that the loss of groups of small disks from the ROS tips accounts for approximately 20% of the total disk turnover. The remaining 80% were shed after the onset of the light cycle.

KEY WORDS membrane turnover · photoreceptor · pigment epithelium · phagocytosis

The light-sensitive outer segments of rod photoreceptors (ROS) are composed of stacks of double-membrane disks surrounded by a plasma membrane (11, 24). The visual pigment, rhodopsin, comprises approximately 80% of the total protein of these ROS membranes (9, 15). Autoradiographic studies with labeled amino acids have established that ROS membranes are renewed throughout life (30). New disks are assembled at the ROS base adjacent to the connecting cilium, and this process displaces previously formed disks farther away from the cell body (27). In animals on cyclic light, the rate at which new disks are added is greater during the light portion of the cycle than in darkness (6, 7).

An optimum ROS length is maintained by the shedding of groups of disks from the ROS tip (29). These detached membrane packets are phagocytized (8, 29) and degraded (19) by the pigment epithelium (PE). ROS shedding occurs shortly after the onset of light (5, 18, 22, 23) which is accompanied by a decrease in ROS length and a loss of rhodopsin (10). When animals entrained to cyclic light are kept in darkness, shedding occurs at a reduced level early in the day, suggesting a free-running, circadian rhythm (7, 22), whereas in constant light, cyclic shedding is abolished and phagosomes are rarely observed in the PE (7, 13).

In this study, we evaluate the effects of temperature on the rate of membrane addition and loss in red rods of *Rana pipiens* tadpoles maintained under cyclic lighting. The rate of membrane addition to the ROS was established by autoradiography after [^{3}H]leucine injection. The rate of membrane loss from the ROS tip was established by monitoring the phagosome content of the PE. Our observations substantiate the previous suggestion (18) that ROS lose membrane disks from their tips in two ways. Large fragments are shed shortly after the onset of the light cycle, whereas small packets of disks are lost throughout the day. Maintenance of tadpoles at progressively higher temperatures affects the rate of disk loss by these two processes differently. By comparing the rate of disk addition with the rate of disk loss as a consequence of light-stimulated shedding, we conclude that detachment of the small disk packets accounts for approximately 20% of the total ROS turnover.

MATERIALS AND METHODS

Animals

Rana pipiens tadpoles were obtained from the Amphibian Facility, University of Michigan, Ann Arbor. Midlarval animals at stages XIII–XVII (26) were selected for use in this study. They were maintained in 19-cm stacking dishes containing 10% Holtfreter's solution (16) in controlled temperature incubators and were fed parboiled spinach. The water was changed and fresh food was added at 2- to 3-day intervals, except for the 33°C maintained group. For these animals, food and water were changed each day. Tadpoles were exposed to 12 h of light followed by 12 h of darkness daily. The light source in each incubator was a 25-W tungsten bulb, which delivered 20 lx of illumination at the level of the animal containers. The lighting intensity was measured with a calibrated PIN photodiode (United Detector Technology Inc., Santa Monica, Calif.). Animals were acclimated to this lighting regimen at the indicated temperatures for at least 7 days before commencement of the sampling schedule and treatments described below.

Tissue Preparation

Eyes were fixed by immersion in a mixture of 2.5% glutaraldehyde, 2% formaldehyde in 0.1 M cacodylate buffer (pH 7.4) containing 0.025 $CaCl_2$ (18). Eyes recovered during the dark portion of the day were excised under dim red light (Wratten number 1 filter, 15 W bulb). After enucleation, eyes were placed in fixative and a small cut was made through the cornea and iris near the limbus to allow fixative penetration. Eyes remained in fixative overnight in the refrigerator. The following morning, the cornea, lens, and iris were cut away, and the posterior hemisphere was transected with a cut along the dorsoventral axis passing through the optic nerve. After a buffer rinse, the tissues were postfixed in 1% osmium tetroxide in 0.1 M cacodylate buffer (pH 7.4) for 90 min. They were quickly dehydrated with a graded ethanol series and were infiltrated with a 1:1 mixture of Epon:propylene oxide. After evaporation of the propylene oxide overnight, tissues were placed in fresh Epon in flat embedding molds. The tissue was carefully oriented before polymerization of

the plastic so that sections could be cut from the block face along the entire expanse of retina and PE from dorsal to ventral margin. Sections 1-μm thick were stained with either Azure II, toluidine blue, or Paragon epoxy tissue stain (Paragon C. and C. Co. Inc., Bronx, N. Y.) for light microscope study.

Selected tissues were thin sectioned for electron microscopy. Sections with a silver diffraction color were picked up on parlodian-coated single-hole grids. After staining with uranyl acetate and lead citrate, the sections were examined in a Siemens Elmiskop 1A.

Autoradiography

Tadpoles received intraperitoneal injections of 25 μCi/animal of L-[(*N*)-4,5-^{3}H]leucine (New England Nuclear, Boston, Mass.; 5 Ci/mmol). Eyes were recovered and fixed by the procedure described above 1, 4, or 6 days later. Plastic sections approximately 1-μm thick were placed on precleaned glass microscope slides. Slides were dipped in Kodak Nuclear Track Emulsion (NTB2) diluted 1:1 with distilled water at 40°C. After drying, slides were stored in airtight bakelite slide boxes containing a desiccant (anhydrous $CaSO_4$). After exposure for 2–3 wk at 4°C, the slides were developed for 2 min in Kodak Dektol diluted 1:1 with distilled water at 15°C. After a distilled water rinse, they were fixed with Kodak Fixer (number 197 1746) for 5 min. Sections were stained through the emulsion for 10–15 s with 1% toluidine blue in 0.07 M phosphate buffer (pH 7.2) at 60°C. After several rinses in distilled water, the autoradiographs were dried, and cover glasses applied with immersion oil.

Culture Procedures

The degradation of phagosomes was followed in PE maintained in vitro in the absence of the retina. Eyes were removed, after 2 h of light exposure, from tadpoles kept at 28°C. After the anterior segment of each eye was carefully removed, retinas were gently teased from the PE which usually remained attached to the outer wall of the eye cup. A clean separation was not always achieved in these light-adapted eyes, and frequently small expanses of PE adhered to the retina or patches of retina remained attached to the PE. These areas were discarded and approximately six to eight strips of PE were obtained from the two eyes of each animal. Pooled tissues from each of five tadpoles were placed in separate compartments in Falcon plastic Petri dishes (number 1009) containing a Ringer's bicarbonate-glucose medium gassed with O_2/CO_2 (95/5%). This medium has previously been utilized for short-term culture of frog retinas (4). Cultures were maintained at 28°C in a constant temperature incubator and were gently rocked on a gyratory platform shaker (40 RPM). PE samples were recovered from each pooled group at the time of isolation and at 2- to 4-h intervals through the following 22 h. These recovery times corresponded to the previous sampling times chosen for our in vivo observations. The remaining tissues were changed to fresh culture medium at each of the recovery times. Fixation and tissue processing followed the same procedures used for the in vivo material described above.

Measurements

All quantitative data from light microscope material were obtained using a 100 × oil immersion objective and 12.5 × ocular lenses. Measurements of PE expanse and phagosome dimensions were made with a calibrated ocular micrometer with 1.3-μm divisions, whereas labeled band displacement was made with a micrometer having 0.5 μm per division. Because phagosomes were irregular in shape, all measurements of these inclusion bodies were of the largest dimension, i.e. length of elongate phagosome profiles, diameter of circular bodies. All measurements of ROS lengths and ^{3}H-band displacement were made exclusively from red rods. ROS shedding frequencies were calculated by using the percentage of the ROS that shed each day as the denominator and 100 as the numerator. The contribution of green rods to the phagosome population of the PE is small, because they represent only 3% of the total rod photoreceptors in the tadpole. Furthermore, because the renewal rate in green rods is lower than the rate in red rods (30), their contribution should be less than the amount predicted by their frequency of occurrence.

RESULTS

Previous studies have established that the ROS shed packets of disks from their tips shortly after the onset of the light cycle (5, 10, 18, 22, 23). These ROS fragments are phagocytized by the adjacent PE and persist for awhile as inclusion bodies within the cytoplasm of the PE cells. These inclusion bodies have been referred to as phagosomes to denote that they are engulfed foreign bodies with an origin different from that of other organelles within the PE (29). We have monitored the phagosome content of the PE in *R. pipiens* tadpoles in order to establish the rate of membrane loss from the adjacent ROS.

Phagosomes within the PE of the tadpole (Figs. 1–4) are virtually identical to those described previously in the adult frog (5, 29). They are highly irregular in shape and size and can be distinguished with light microscopy from other organelles by their high affinity for the cationic stains. They have a deep rose hue when stained with Paragon, and color a deep blue with Azure II or toluidine blue. They stain more intensely than the rhomboid- to circular-shaped myeloid bodies. Melanosomes are brown, and their paracrystalline structure causes light scattering as the

sections are moved through the lens focal plane. Inasmuch as phagosomes do not scatter light, those inclusion bodies with dimensions similar to those of melanosomes can be recognized even when located in the melanosome-filled cytoplasm along the apical border of the PE. Many phagosomes have small circular profiles <2 μm in diameter, whereas others are rectangular to elliptical, are similar in width to ROS (4–6 μm), and reach 10 μm and more in length. We determined the number and size of these densely staining inclusion bodies at selected intervals throughout the day in animals kept in cyclic light (12L:12D) at 23°, 28°, and 33°C (Fig. 5).

At the beginning of the day (time 0), just before the onset of light, the most prominent phagosomes at each temperature were <2 μm in size. After the onset of light, phagosomes >2 μm in size increased in number, reaching a maximum by 2–4 h (Figs. 1–4 and 5). Phagosomes between 3.3–4.6 μm in size were the most frequent, though a few were present with lengths between 9.8 and 11.1 μm. A bimodal distribution of phagosome sizes was evident in the data from the samples taken during the first few hours of the day. The smallest size group accounted for most of those present before the onset of the light, whereas the newly arriving phagosomes were larger. After 8 h, phagosomes in the larger-size categories, which were numerous in the 2- to 4-h samples, were absent. The larger phagosomes continued to disappear, and by the end of the light cycle (12-h sample) and throughout the remainder of the day the histograms showed a population of phagosomes essentially identical to those present before the onset of light.

Though it is evident in Fig. 5 that more phagosomes were present at higher temperatures, this is more readily visualized when total counts at each of the recovery times are considered. Because the histograms showed that the number of densely staining inclusion bodies <2 μm in size changed little throughout the day but that the number of those with larger dimensions increased after light exposure, we separated the phagosome counts into these two size categories and plotted the data as a function of time (Fig. 6). In the descriptions that follow, phagosomes 2 μm and less in size are referred to as small phagosomes and those 2 μm and more in size as large phagosomes.

As can be seen in Fig. 6 A, there was an abrupt increase in the number of large phagosomes after light exposure. Large phagosomes reach highest counts at 2 h in the 23° and 33°C groups, whereas this level was reached at 4 h in the 28°C animals. Thereafter, the number of large phagosomes declined to the approximate level seen before light exposure at around 12 h into the day.

It is also evident in Fig. 6 A that the number of large phagosomes increased when tadpoles were maintained at progressively higher temperatures, though this increase was not precisely linear. The mean counts of large phagosomes at the peak response times show a 1.8-fold increase over the temperature range of 23°–28°C as compared to a 1.2-fold increase with temperature elevation from 28° to 33°C. The temperature coefficient (Q_{10}) of production of large phagosomes over the entire range of 23°–33°C was 2.2, whereas the Q_{10} calculated over the ranges of 23°–28°C and 28°–33°C were 3.4 and 1.4, respectively.

Counts of small phagosomes though somewhat variable show no clear changes in response to light (Fig. 6 B). It was evident, however, that the counts of small phagosomes were slightly higher at higher temperatures. Because the numbers of small phagosomes change little throughout the day, we pooled all the counts during the day for each of the temperature groups to obtain a mean number of small phagosomes. The average counts of small phagosomes at each of the three temperatures were: 23°C–13.6 ± 0.8; 28°C–16.1 ± 1.0, and 33°C–18.1 ± 0.8 small phagosomes/1,000-μm PE (mean ± standard error). These differences indicate a 1.18-fold increase with temperature elevation from 23° to 28°C and a 1.12-fold increase with temperature elevation from 28° to 33°C. The overall Q_{10} of small phagosome production with increases from 23° to 33°C was 1.3, whereas the 23°–28°C and 28°–33°C means reflect a Q_{10} of 1.4 and 1.3, respectively.

It is evident from these comparisons that large phagosomes increase in number to a greater extent than do the small phagosomes at progressively higher temperatures. Though all these structures appear virtually identical with light microscopy, it is possible that these differential responses to temperature may reflect different origins for the components of these two size categories. Although it has been previously suggested that the densely staining particles of various shapes and sizes represent different stages in the degradation of phagocytized debris (5, 29), it is possible that at least some of the structures <2 μm in size may represent components of the PE

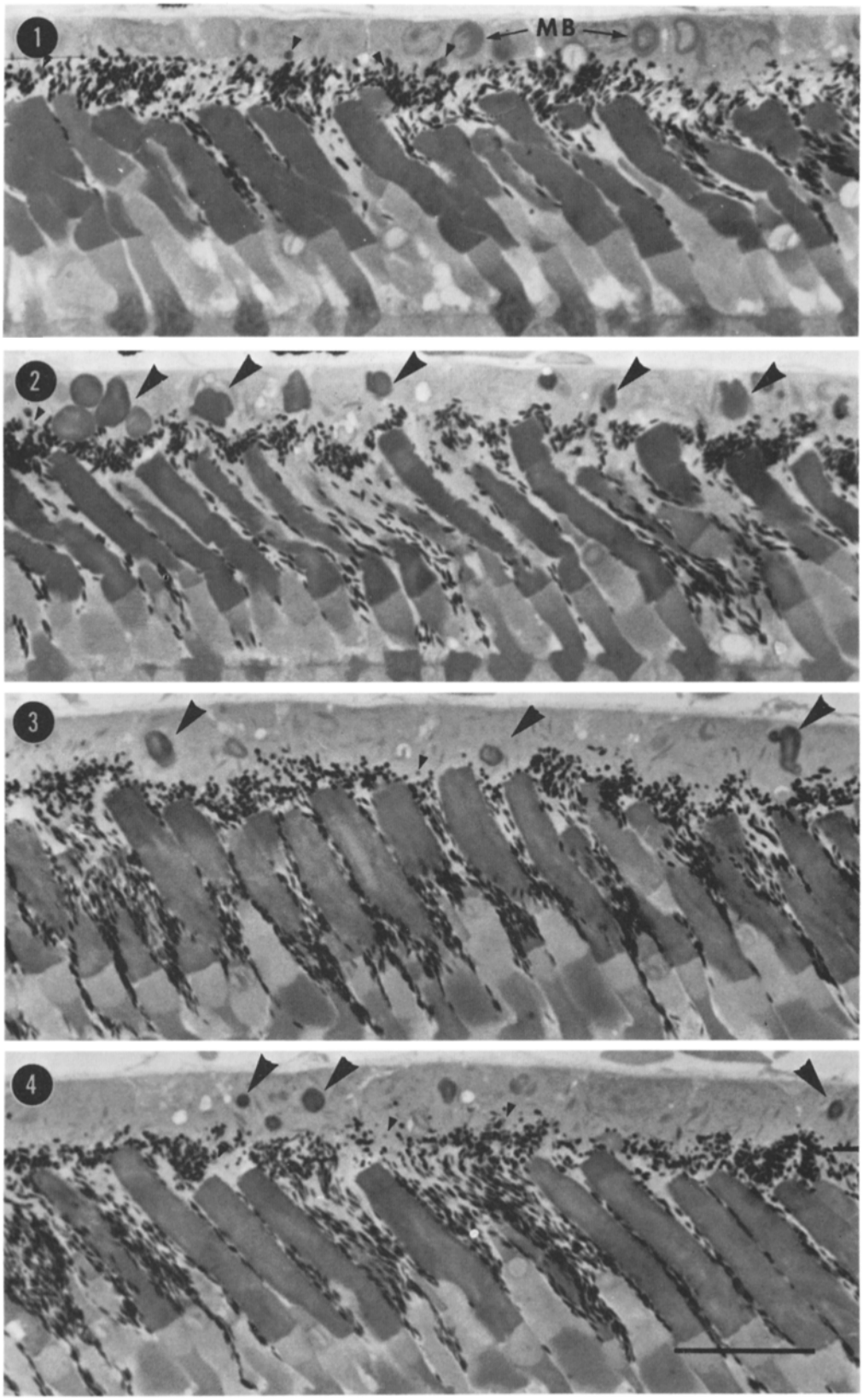
1
MB
2
3
4

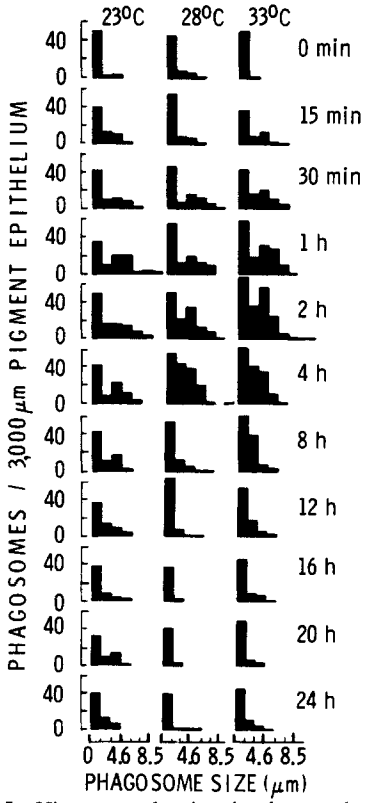

FIGURE 5 Histograms showing the changes throughout the day in the size and number of phagosomes in the PE of tadpoles maintained at the indicated temperatures. Dimensions along the abscissa reflect major axis (length) of phagosomes with elongate profiles or diameter of phagosomes with circular profiles. Phagosome-size bins from left to right along the abscissa represent dimensions 0–2 μm, >2–3.3 μm, >3.3–4.6 μm, >4.6–5.9 μm, >5.9–7.2 μm, >7.2–8.5 μm, >8.5–9.8 μm, and >9.8–11.1 μm. The lights were on after the time-zero sample and were off at 12 h. Eyes were fixed in the dark at 0-, 16-, 20-, and 24-h sampling times. Phagosomes <2 μm in size are present throughout the day in relatively constant numbers within each temperature group. Phagosomes >2 μm in size increase after light exposure and are present in greater numbers at the higher temperatures. See text for more detailed description.

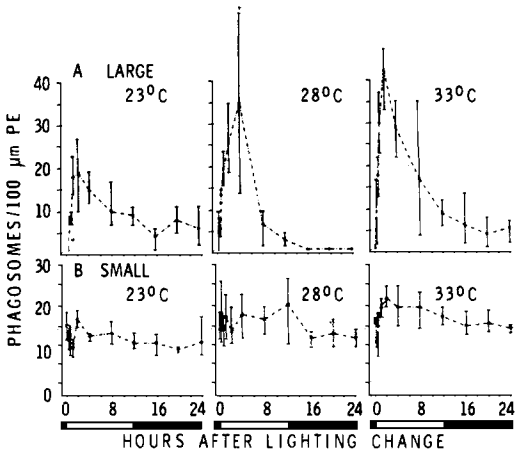

FIGURE 6 Variations in the number of phagosomes within the PE throughout the day in relationship to cyclic lighting. Large-phagosome plots (upper) refer to phagosomes >2 μm in size. Small-phagosome plots (lower) refer to phagosomes below <2 μm in size. Bars around means are range lines. Means at each recovery time reflect counts from one eye from each of three animals, except for the 15- and 30-min samples where counts are from one eye from each of two animals. Note that the large phagosomes are numerous during the first few hours of the light cycle. Also note that progressively more large phagosomes are present during this period when animals are raised at higher temperatures. In contrast, small-phagosome counts do not show wide fluctuations during the day though counts are slightly higher in the light during the first 12 h than during the remainder of the day in darkness.

cells that are undergoing autophagy. To evaluate in greater detail the morphological features of all the densely staining inclusion bodies, eyes fixed at selected intervals throughout the day were sectioned for ultrastructural analysis.

In eyes recovered 15 min–1 h after light exposure, large packets of membrane material possessing all the characteristics of ROS disks were observed within the PE. These phagosomes were composed of stacks of double membranes with bulbous swellings at the lateral margins of the

FIGURES 1–4 Photoreceptor-PE complex in *R. pipiens* tadpoles maintained at 28°C. The PE is at the upper border of each micrograph. In eyes recovered before the onset of the light cycle (Fig. 1), only small profiles of densely staining phagosomes are present in the PE (small arrowheads). Note melanosomes in the dark-adapted position. (*MB*) myeloid bodies. In eyes fixed 2 h after the onset of the light cycle (Fig. 2), the PE contains numerous profiles of large, recently shed, phagosomes (large arrowheads). A small phagosome (small arrowhead) is also present. Note that melanosomes are now in the light-adapted position. In eyes fixed later in the day, phagosomes are reduced in number and size. 8-h recovery eye (Fig. 3) and 12-h recovery eye (Fig. 4). Bar for Figs. 1–4, 20 μm. See text for further explanation.

double membrane leaflets, a characteristic of ROS. They differed from subjacent ROS membranes only by having a greater affinity for the uranium and lead salts (Fig. 7). Many of these phagosomes were rectangular in shape at these early recovery times and were located near the ROS tips. The number of disks was determined in well-oriented phagosomes in eyes recovered 1 h after light exposure for each of the temperature groups. Though disk counts ranged from 102 to 194 per phagosome, the mean number of disks per phagosome at each temperature was similar (23°C-139.5 ± 5.7; 28°C-129.9 ± 7.6; 33°C-129.9 ± 4.8; mean ± standard error). In the PE recovered 2 and 4 h into the light cycle, the membrane composition of the large phagosomes remained distinct though their disk margins were greatly distended (Fig. 8). The peripheries of many of the large phagosomes during this recovery period had rounded to crenulated contours.

The largest phagosomes observed in the PE in the 8- and 12-h samples were reduced in size compared with those observed earlier in the day. Though the membranous composition of these phagosomes could be recognized in many of the sections, the membranes were obscure in some areas where they merged with patches of high electron density (Fig. 9). A granular material of intermediate electron density was occasionally present at the periphery of some of the large phagosomes in material recovered at intervals of 1-16 h. This material was confluent with the outer edge of membrane debris and was located within the confines of the periphagosomal membrane (Fig. 13). Sometimes present within this granular matrix were circular profiles 0.10-0.15 μm in size. A similar membrane-bound granular material, free of associated ROS disk debris, was a common feature within the PE at each recovery time examined. These granular bodies also contained circular profiles which were sometimes arranged in a highly organized, hexagonal array (Fig. 14).

Numerous examples of membrane debris in the PE identical in size to the structures that we classified as small phagosomes with light microscopy were evident at each sample time studied by electron microscopy (Figs. 7, 10, 11, 12, 17, 18). These small packets of electron-dense, membranous material were located in the mid-to-basal region of the cells as well as within the apical cytoplasm. Though some of these structures could have been degraded from larger particles, another possible source of this material was suggested by the configuration of membrane disks at the ROS tips. In many of the ROS in eyes recovered at each sample time, the apical disks were curled into configurations suggesting stages in the detachment of these small disk groups (Figs. 7, 15-17). The number of disk profiles observed in these whorls ranged from 4 to 37. Small packets of membrane debris within the apical cytoplasm of the PE in close proximity to ROS tips were also observed (Figs. 7, 17-18).

The observed stability of the small-phagosome population could be the result of loss of small packets of disks from ROS tips at a relatively constant rate throughout the day, an idea based on the assumption that degradation of large phagosomes to a smaller size contributes little to the small-phagosome population. This suggests that if the retina were removed from the PE, the small phagosomes already present would be degraded and their numbers reduced because the source of the small phagosomes would no longer be present. Alternatively, if the structures that we have classified as small phagosomes represent the continued autophagy of membrane material produced by the PE cells, then the removal of the retina should have little effect on this population of inclusion bodies. To test these possibilities, we separated the retina from the PE, maintaining the latter in vitro for subsequent sampling and microscope analysis.

Eyes were removed from five tadpoles maintained at 28°C, 2 h after the onset of light. This recovery time was chosen so that the PE could contain both small phagosomes and recently interiorized large phagosomes. Because we knew the pattern of degradation of large phagosomes at this temperature from our in vivo studies (Fig. 6 A), we could compare directly any variations in the temporal pattern of degradation in this in vitro experiment.

The counts of large and small phagosomes from our in vitro experiment (Fig. 19) are presented superimposed on the counts of phagosomes from the 28°C in vivo recovery eyes previously presented in Fig. 6. As is evident in Fig. 19 A, the numbers of large phagosomes in the isolated PE sample recovered at the time of isolation (2 h into the light cycle) are similar to the numbers observed in vivo at the equivalent recovery time. In the second sample recovered after 2 h in vitro (4 h into the light cycle), the number of large

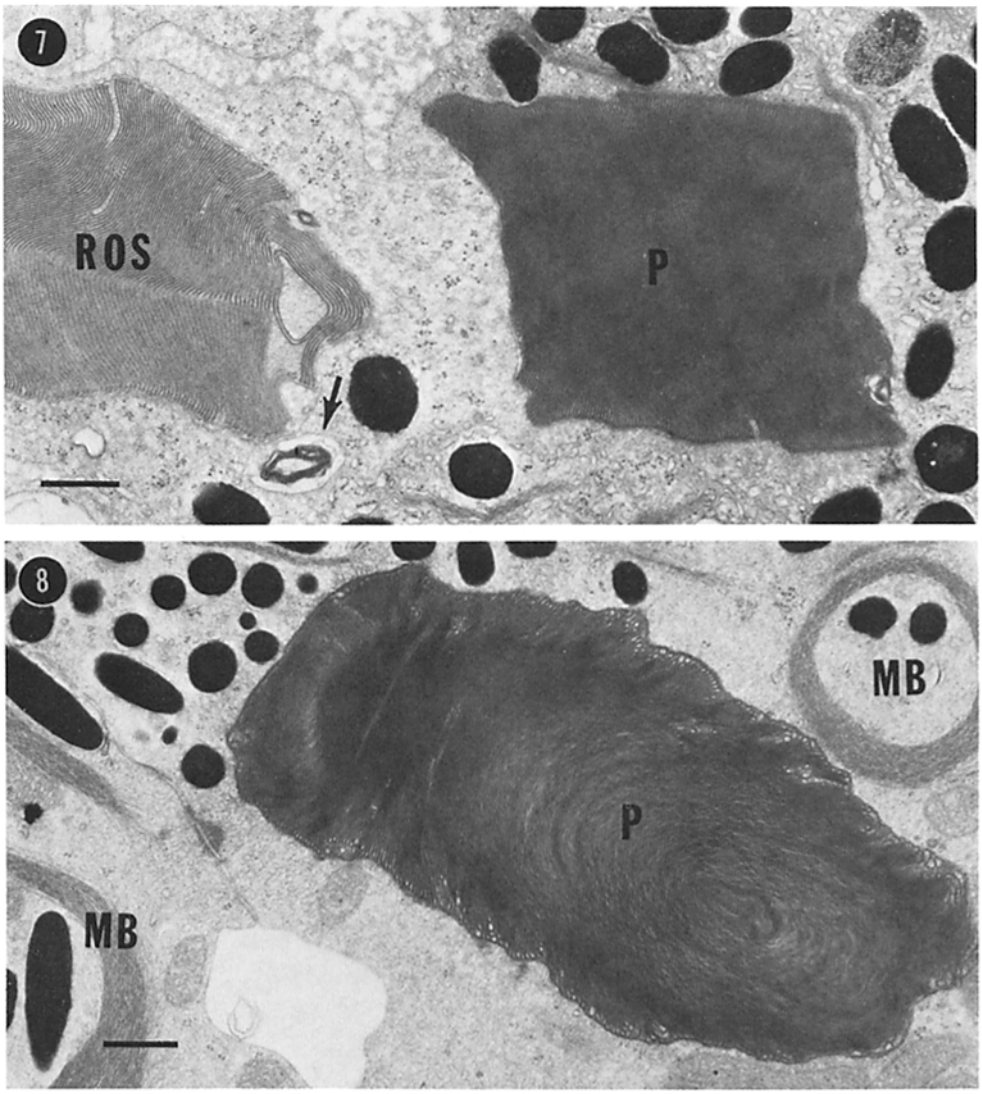

FIGURE 7 A large phagosome (*P*) approx. 5 μm long, composed of 127 membrane disks, within the PE in close proximity to the tip of a rod outer segment (*ROS*). This eye was recovered 15 min into the light cycle from a tadpole maintained at 28°C. Note the irregular disks at the *ROS* tip and the small packet of electron-dense membranous material at arrow. Bar, 1 μm.

FIGURE 8 Large phagosome (*P*) approx. 9 μm long, composed of 174 membrane disks, in the PE of an eye recovered 1 h into the light cycle from a tadpole maintained at 28°C. The individual disks are distinct but the disk edges are swollen and vesiculated along the periphery of the phagosome. Cf. phagosome periphery in Fig. 7. (*MB*) myeloid bodies. Bar, 1 μm.

phagosomes was reduced by approximately one-half of that observed 2 h earlier. This is in contrast to the continued increase in the number of large phagosomes in vivo. Apparently, in the tadpole, ROS shedding and phagocytosis by the PE continued after 2 h, resulting in the continued increase in the number of large phagosomes, whereas in the in vitro preparations the source of the large phagosomes was no longer present and many of the phagosomes present at the time of PE isolation were degraded. Degradation continued and the counts of large phagosomes, in vivo and in

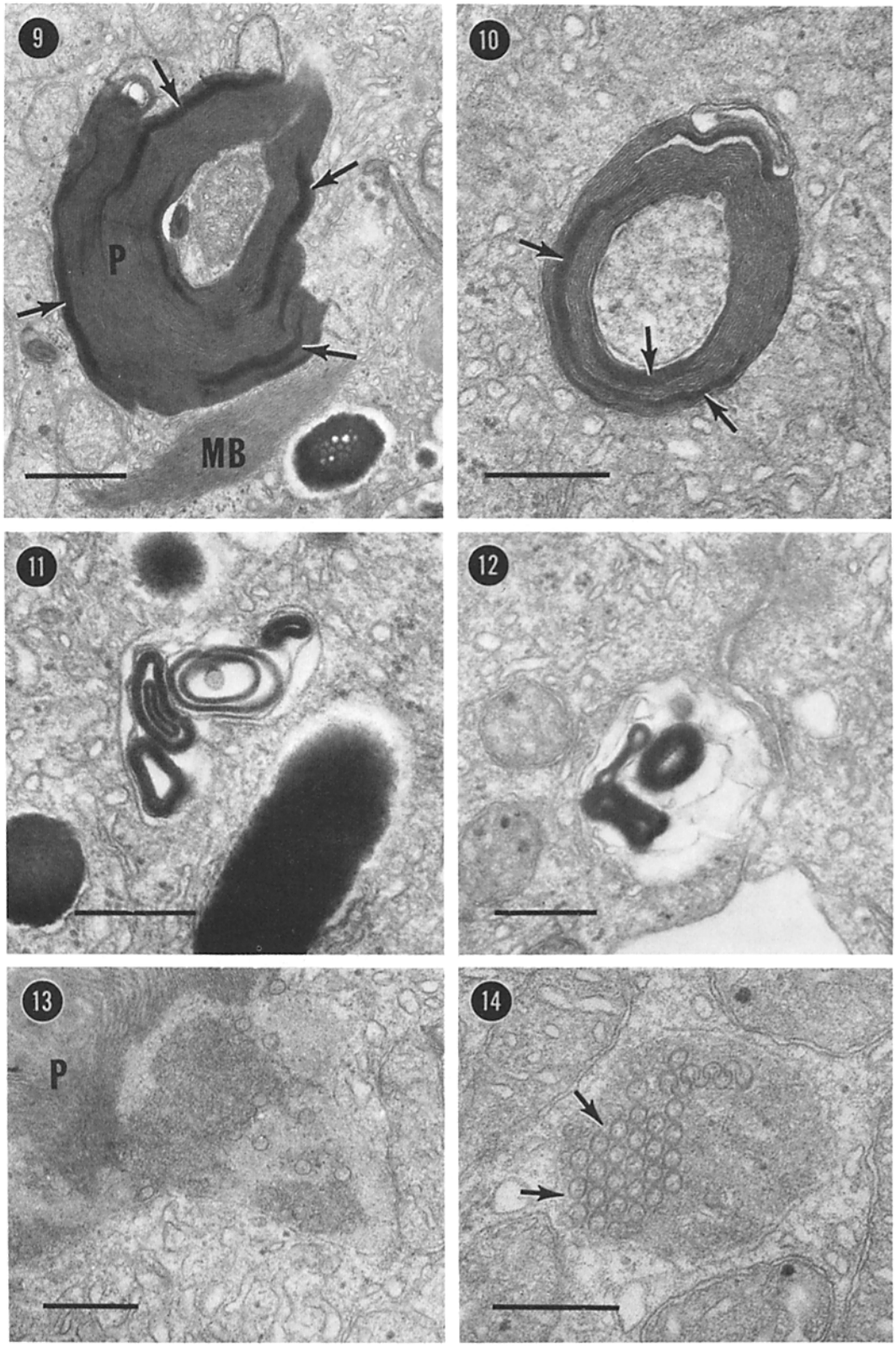
9
P
MB
10
11
12
13
P
14

vitro, were virtually identical at the 8- and 12-h recovery times.

The numbers of small phagosomes (Fig. 19 B) in the in vitro samples recovered at the time of isolation (2 h into the light cycle) were similar to the number of small phagosomes observed in vivo at the equivalent recovery time. However, the numbers of small phagosomes present after isolation to culture progressively decreased at successive sampling times. This was in sharp contrast to the numbers of small phagosomes in vivo, which showed a slight increase at equivalent times. The temporal pattern in the degradation of small phagosomes in vitro was similar to that of large phagosomes both in vitro and in vivo. The loss from the PE of these small, densely staining inclusion bodies after removal of the retina indicates that the ROS are the source of these structures. Furthermore, the disappearance of the large phagosomes from the cultured PE without a concomitant increase in the number of small phagosomes indicates that incompletely degraded, large phagosomes are not the source of small phagosomes.

These observations implicate the ROS as the cell that is responsible for the production of the membrane debris present in both large and small phagosomes. The ROS membranes present in large phagosomes are lost in response to the onset of the light cycle, whereas most of the membrane debris present in small phagosomes appears to result from the shedding of small groups of disks throughout the day. What is the relative importance of these two methods of ROS disk loss? This can be determined with knowledge of both the rate of disk loss and the rate of disk addition. To maintain a stable ROS length, the rate of disk loss must be equal to the rate of disk addition. In ROS that are increasing in length, the rate of disk addition must be greater than the rate of disk loss.

To determine whether tadpole ROS increase in length during the stages utilized in these studies, eyes from 37 animals representing all stages between XIII and XVII were selected for measurements of ROS. These eyes were taken from animals maintained at 23°, 28° and 33°C. The lengths of 10 well-oriented outer segments were measured from the posterior region in each eye. An initial analysis of the data revealed no differences that could be attributed to temperature. Therefore, the data from all specimens at the same stage were pooled. The results of these measurements (Table I) show that the mean of ROS length from the individual animals ranges from a low of 24.7 μm at stage XVII to a high of 32.0 μm at stage XVI, a difference of 7.3 μm. Despite this variability, the combined ROS means through these stages are not significantly different. Thus, ROS do not show a net increase in length during the stages utilized in these studies.

The renewal rate of ROS in tadpoles maintained at the three temperatures was determined

FIGURE 9 Phagosome profile (*P*) approx. 3 μm in diameter from a 12-h recovery eye. The membranous composition is distinct throughout most of body at the phagosome except in the regions indicated by arrows. (*MB*) myeloid body. Bar, 1 μm.

FIGURE 10 Phagosome approx. 1 μm in diameter, composed of approx. 20 membrane lamina, from an eye fixed 12 h into the day. The membranes are distinct over most of the phagosome profiles except in the highly electron-dense regions indicated by arrows. Bar, 0.5 μm.

FIGURE 11 Small profile of membranous material in the PE from a 28°C tadpole recovered 20 h into the day. Though the membranous nature of this material is evident, its electron density nearly matches that of adjacent melanosomes. Bar, 0.5 μm.

FIGURE 12 Small packet of highly electron-dense membranous material near the lateral border of a PE cell from a 28°C tadpole eye recovered at 20 h. Bar, 0.5 μm.

FIGURE 13 Portion of a phagosome (*P*) from a 28°C tadpole eye recovered at 16 h. Membranous material is evident in upper left but merges with a granular material with two electron densities near the center of the micrograph. Small circular profiles 0.1–0.15 μm in diameter are present within this granular structure. Bar, 0.5 μm.

FIGURE 14 Membrane-surrounded profile of granular material in the PE of a 23°C tadpole eye recovered 15 min after the onset of the light cycle. Numerous circular profiles similar to those shown in Fig. 13 are closely packed within this structure (arrows). Bar, 0.5 μm.

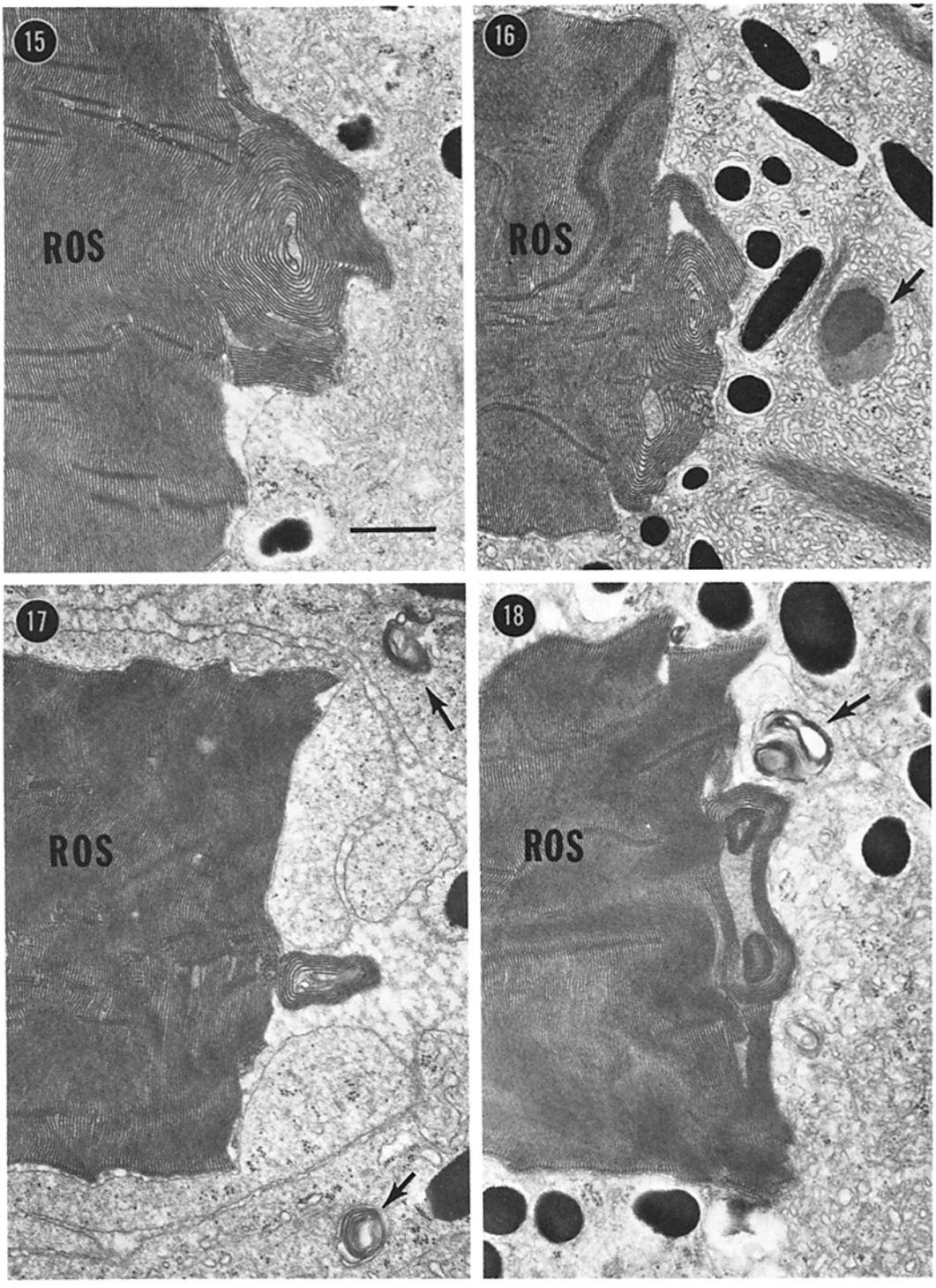
15
ROS
16
ROS
17
ROS
18
ROS

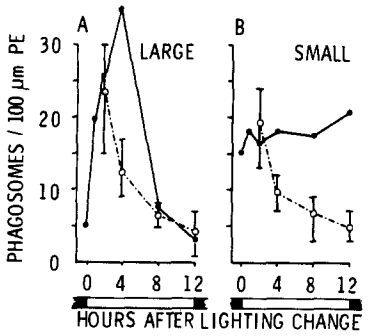

FIGURE 19 Phagosome counts in the PE isolated to culture 2 h after light exposure from *R. pipiens* tadpoles maintained at 28°C. Open circles (○) are the means from three samples. Bars around sample means are range lines. Closed circles (●) are phagosome counts from 28°C in vivo material presented in Fig. 6. Both large and small phagosomes are degraded under these conditions. See text for further explanation.

by light microscope autoradiography after [^{3}H]leucine injections. These data are summarized in Table II, and autoradiographs of this material are presented in Figs. 20–22. Because the tadpole ROS contain 35.6 + 0.35 (mean ± standard error) disks per micrometer ROS length, the rates of ^{3}H-band displacement of 0.91, 1.57, and 1.84 μm/day at respective temperatures of 23°, 28°, and 33°C correspond to the addition of 32.4, 55.9, and 65.5 ROS disks/day.

Because each large phagosome present in the PE at the maximum response time is the result of a single shedding event by a rod in the subjacent retina (5, 18, 22, 23), with information on rod density we can calculate the percentage of rods that shed each day. From counts of ROS in eyes from three animals at each of the different temperatures, a density of 104.8 ± 1.02 ROS/1,000 μm of retina was obtained. The numbers of large phagosomes/1,000 μm PE at the peak response times shown in Fig. 6 A are: 19 at 23°C, 35 at 28°C, and 42 at 33°C. Therefore, 18, 33, and 40% of the ROS shed each day at these respective temperatures. From these ROS shedding frequencies, the average interval between repeated sheddings was determined. These calculations indicate that each rod sheds every 5.6 days at 23°C, every 3 days at 28°C, and every 2.5 days at 33°C. From

TABLE I

Outer Segment Length (μm) in Red Rods of Rana pipiens Tadpoles

Stage	Number of animals	Mean length	(±Standard error)	Range of specimen means
XIII	5	27.2	(±0.4)	25.8–27.7
XIV	11	28.3	(±0.5)	25.8–31.6
XV	8	27.9	(±0.6)	24.9–30.0
XVI	5	28.7	(±0.9)	27.3–32.0
XVII	3	27.3	(±1.5)	24.7–29.9

ROS lengths in *Rana pipiens* tadpoles at the indicated stages. Measurements were made of 10 ROS from the posterior pole of eyes fixed 1–2 h after the onset of the light cycle.

TABLE II

Renewal Rates for ROS in Rana pipiens Tadpoles

Temperature	^{3}H-band position		Renewal rate (R)
	Day 1 (t_1)	Day 4 (t_2)	
°C	μm		μm/day
23	1.44 ± 0.12	4.16 ± 0.14	0.91
28	1.96 ± 0.02	6.68 ± 0.67	1.57
33	2.46 ± 0.22	7.97 ± 0.39	1.84

Renewal rates (R) for ROS calculated by the formula $R = \frac{Bt_2 - Bt_1}{t_2 - t_1}$ where B is the position of the ^{3}H-band (measured in micrometers from the base of the ROS to the scleral edge of the ^{3}H-band; see Figs. 20–22) and t is the elapsed time after injection of [^{3}H]leucine.

FIGURE 15 Rod outer segment (*ROS*) tip from a 28°C tadpole eye recovered 12 h into the day. A circular array of approx. 15 *ROS* disks indent the apical surface of the PE. Bar, 1 μm.

FIGURE 16 Rod outer segment (*ROS*) tip from a 28°C tadpole eye recovered 1 h after the beginning of the light cycle. Note the irregular configuration of the apical disks suggesting a possible stage of detachment. A small profile of a membrane-bound particle containing granular material of two electron densities is present within the PE cell (arrow).

FIGURE 17 Rod outer segment (*ROS*) tip from a 28°C tadpole eye recovered 15 min after the onset of the light cycle. Note the small whorls of six *ROS* disks in possible stage of detachment from the *ROS* tip. Two profiles of membranous material (arrows) are present within the adjacent PE.

FIGURE 18 Rod outer segment (*ROS*) tip from a 23°C tadpole eye recovered 8 h into the light cycle. The apical disks are in an irregular configuration, and a profile of membranous material (arrow) is present in the adjacent PE cell.

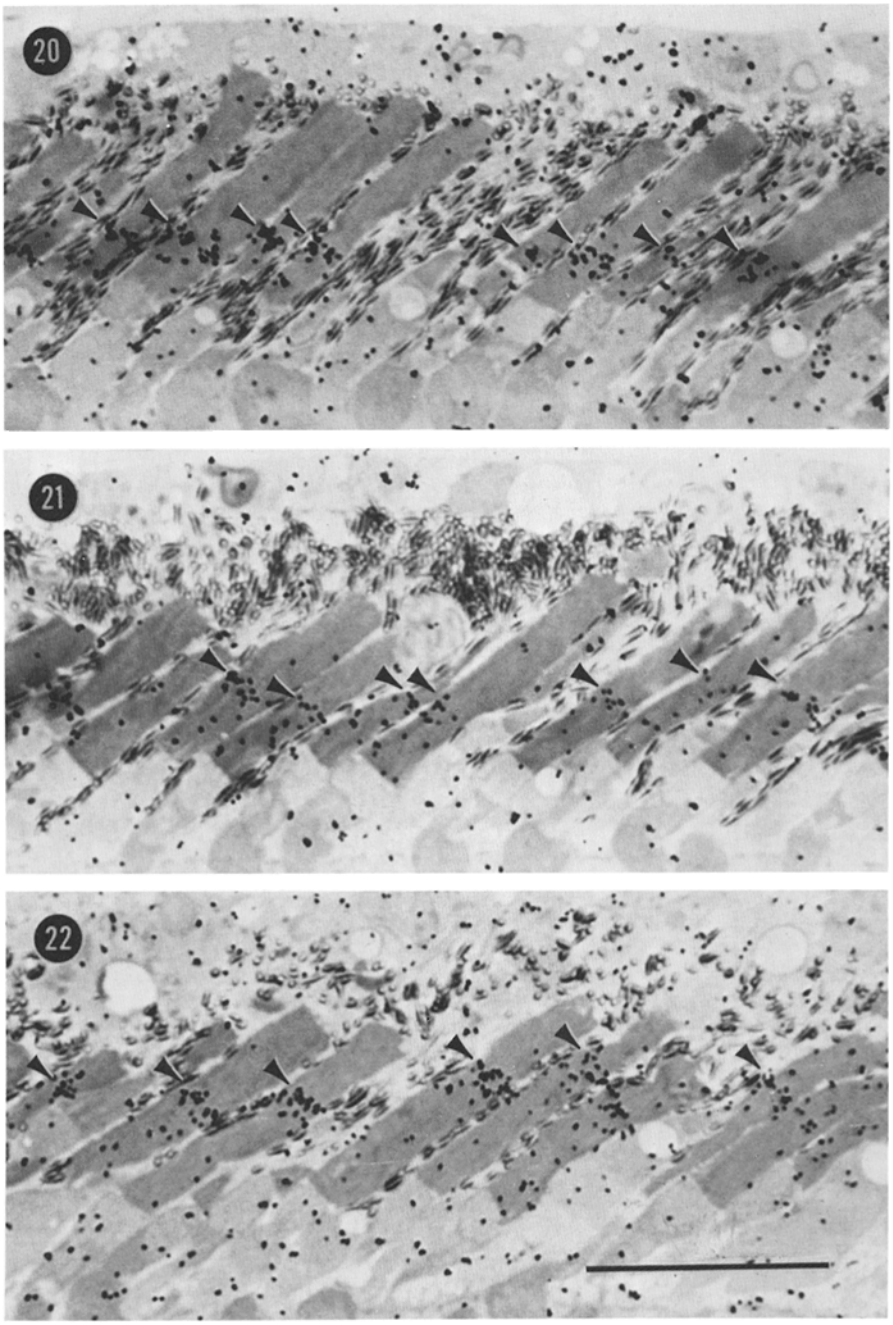

FIGURES 20–22 Autoradiographs of the photoreceptor-PE complex in mid-larval *R. pipiens* injected with [^{3}H]leucine 6 days before fixation.

FIGURE 20 Stage XVI tadpole maintained at 23°C.

FIGURE 21 Stage XIII tadpole maintained at 28°C.

FIGURE 22 Stage XIII tadpole maintained at 33°C. Note that the bands of silver grains (arrows) are located farther away from the ROS base in the animals maintained at higher temperatures. Bar, 20 μm.

our renewal data, we know that in 5.6 days, 181.5 disks will be added to ROS in tadpoles maintained at 23°C; in 3 days, 167.7 disks will be added to ROS in animals maintained at 28°C; and in 2.5 days, 160.2 disks will be added to ROS in tadpoles maintained at 33°C. The average number of disks lost in response to light stimulation is reflected in the number of disks present in large phagosomes of the PE. Because our disk counts in large phagosomes were made on material fixed shortly after the onset of the light cycle before any detectable loss of disks on account of degradation, these numbers should closely represent the average number of disks lost from ROS at the beginning of the light cycle.

In animals maintained at each of the three temperatures, the average number of disks present in large phagosomes was less than the number of disks added at the ROS base in the time interval since the previous light-induced shedding. As ROS show no net increase in length during the tadpole stages utilized, these excess disks must represent those small packets of membrane debris which we classified as small phagosomes and which are apparently lost from ROS throughout the day. These data are summarized in Table III.

DISCUSSION

The observations in this study indicate that there are two methods by which disks are lost from ROS. Large disk packets are shed after the onset of the light cycle. These fragments are subsequently phagocytized by the PE, which results in an elevation in the number of large phagosomes in this tissue. Phagosomes are present in highest concentration 2–4 h into the light cycle and are degraded by 8–12 h.

The disks lost in response to light, however, account for only about 80% of the total disks added between shedding events at each of the temperatures utilized. Because the ROS do not increase in length during the tadpole stages studied, the remaining disks must be eliminated in some other manner. The apical disks with curled profiles on ROS, suggesting stages of detachment of small disk groups which we observed throughout the day, represents a possible method by which the extra disks are eliminated. If these small disk groups were lost and degraded at a relatively constant rate, this would account for the relatively stable numbers of small phagosomes that we have observed. The finding that small phagosomes disappear from the PE after removal of the retina indicates that they can be degraded and further implicates the retina as the source of the inclusion bodies. The stability in the small-phagosome counts during the period when large phagosomes are decreasing in number indicates that incompletely degraded large phagosomes contribute relatively little to the small phagosome population. Apparently, as large phagosomes are degraded to smaller sizes they make the transition to the lightly staining granular structures thought to represent the end product of degradation (i.e. residual bodies; reference 25) before they decrease in diameter to <2 μm.

Some of the structures that we have counted as small phagosomes may represent grazing sections along the periphery of larger phagosomes which lie above or below the plane of section. It is well recognized that when measurements of structures within sectioned tissues are utilized to establish size-frequency distributions, the observed counts in the smaller size bins will tend to be an overesti-

TABLE III

Summary of Disk Addition and Loss in Red Rods of Rana pipiens Tadpoles

	Temperature		
	23°C	28°C	33°C
(A) ^{3}H-band displacement micrometers/day	0.91	1.57	1.84
(B) Disks added/day (35.6 × A)	32.4	55.9	65.5
(C) Percent ROS shedding/day	18%	33%	40%
(D) Interval (days) between repeated shedding (100/C)	5.6	3.0	2.5
(E) Disks added between sheddings (B × D)	181.4	167.7	160.2
(F) Disks/large phagosome	139.5	129.4	129.9
(G) Difference between disks added and those present in large phagosomes (E-F)	41.9	38.3	30.3
(H) Percent of disks not accounted for in large phagosomes (G/E × 100)	23.1%	22.8%	18.9%

mation of the absolute numbers present. Because of this problem, it is the usual practice in morphometric studies of this nature to correct for this overestimation (1, 12, 14). The correction factors utilized for these adjustments, however, require that the structures under consideration have a circular to oval shape with a relatively uniform diameter. Because phagosomes in the PE are highly irregular in shape and their sizes range from <1 μm in diameter to >10 μm in length, they do not meet this requirement, and we were unable to apply these correction factors to our data.

It is possible that some of the small phagosomes in the PE could be derived from cone outer segments (COS). The diameter of COS tips in the tadpole is 1.5–2 μm. If these tips were shed and ingested by the PE, they would undoubtedly have contributed to the small-phagosome population. Though cone shedding has been well established in squirrels (2) and man (17), recent studies of the goldfish retina indicate that cone shedding occurs shortly after the beginning of the dark cycle (31). Our fixation times during this period were at the beginning of the dark cycle and 4 h later (16-h sample). Because we observed no elevation in the number of small (or large) phagosomes at these sample times, if cones shed in the tadpole early into the dark cycle as in the goldfish, it is likely that cone shedding was initiated, phagocytosis followed, and degradation was completed in the interval between our 12- and 16-h samples.

What factors mediate the loss of large disk fragments from ROS after light exposure? Though an answer to this question must await further studies, several lines of evidence suggest the involvement of an endogenous circadian mechanism. When rats (23) and *Xenopus* tadpoles (7) trained to cyclic light are maintained in continuous darkness, shedding occurs early in the day but at slightly reduced rates. When *Xenopus* tadpoles (7) and adult *Rana* (13) are maintained under low levels of continuous light for 3–10 days, shedding is greatly reduced. Many circadian phenomena are regulated by cyclic changes in serotonin-melatonin metabolism in the pineal gland. In animals on cyclic light, the pineal gland output of melatonin is high during the dark portion of the cycle and low in the light. This fluctuation in melatonin synthesis continues as a free-running circadian rhythm in animals maintained in darkness but is abolished when animals are maintained in continuous light (20). The involvement of the pineal gland in the control of ROS shedding is suggested by the observation that shedding is reduced after light exposure when rats are treated with reserpine, a drug that abolishes some circadian rhythms through its action on the pineal gland (22). In the adult frog, the pineal gland does not appear to be involved in this process because shedding of large ROS fragments will occur in pinealectomized animals after light exposure (13). This result, however, does not rule out the control of ROS shedding by serotonin-melatonin because the enzymes of this pathway are known to be present within the eye (3).

The apparent sustained loss of small disk packets from ROS throughout the day rather than after the onset of the light cycle suggests that different control mechanisms may regulate these two processes. The small groups of ROS disks may be lost in response to a basic instability of the large expanse of apical membrane at the ROS tips. The instability of ROS membranes is suggested by their tendency to fragment when the retina and PE are separated (21). The observations in this study of terminal disks with curled and folded configurations further support this suggestion. Though the loss of these small disk packets may occur in a random manner throughout the day, if these discs were retained the ROS would increase in length. Our measurements indicate that the ROS lengths average 27.9 μm in the tadpole and show no net increase during the stages utilized. We have observed similar lengths in juvenile frogs, but in adults the ROS are around 45 μm long (5). If the rate of loss of small fragments from the ROS tips were reduced during maturation after metamorphosis, the retention of this disk material would provide a mechanism for increasing the ROS length without changing the rate of disk addition or modifying the number of disks lost after light-induced shedding. Our data indicate that the retention of these disks would result in an increase in ROS length by approximately 1 μm during the interval between repeated shedding events.

The temperature coefficient (Q_{10}) of membrane addition to ROS calculated from the ^{3}H-band displacement rates at 23° and 33°C was 2.0, whereas the 23°–28°C and 28°–33°C displacement rates reflect a Q_{10} of 2.5 and 1.4, respectively. This failure of the rods to maintain a linear rate of renewal over the entire temperature range indicates that our higher temperature is above the

normal range for maintenance of the tadpoles. Similar effects of temperatures above 30°C on rates of rhodopsin biosynthesis in isolated frog retinas have been reported previously (4).

It is of interest that the Q_{10} of disk addition and the Q_{10} of large-phagosome production (presented in Results) are similar through equivalent temperature ranges. This suggests a close coupling in the control mechanisms regulating disk addition and loss. However, as documented in the accompanying paper (7), when animals are maintained under different lighting regimes, these two processes can be manipulated independently. The rate of disk addition is greatest in constant light, whereas the frequency of shedding of large disk packets is greatest in cyclic light. Our studies indicate that conditions of cyclic lighting play a fundamental role in the control of membrane turnover in ROS.

The authors are indebted to Ms. Eva Helvacian for her assistance in sectioning the mountains of blocks analyzed in this and the accompanying study.

Dr. Hollyfield was supported by National Institutes of Health research grants EY 00624, EY 01632, Research Career Development Award EY 00023, and by a grant from Fight for Sight, Inc. Dr. Besharse was the recipient of a National Research Service Award, EY 05119.

Received for publication 25 April 1977, and in revised form 25 July 1977.

REFERENCES

1. Abercrombie, M. 1946. Estimation of nuclear population from microtome sections. *Anat. Rec.* **94:**239–247.
2. Anderson, D. H., and S. K. Fisher. 1976. The photoreceptors of diurnal squirrels: outer segment structure, disc shedding and protein renewal. *J. Ultrastruct. Res.* **55:**119–141.
3. Baker, P. C., W. B. Quay, and J. Axelrod. 1965. Development of hydroxyindole-*O*-methyl transferase activity in eye and brain of the amphibian, *Xenopus laevis*. *Life Sci.* **4:**1981–1987.
4. Basinger, S., and M. O. Hall. 1973. Rhodopsin biosynthesis *in vitro*. *Biochemistry.* **12:**1996–2003.
5. Basinger, S., R. Hoffman, and M. Matthes. 1976. Photoreceptor shedding is initiated by light in the frog retina. *Science (Wash. D. C.).* **194:** 1074–1076.
6. Besharse, J. C., J. G. Hollyfield, and M. E. Rayborn. 1977. Photoreceptor outer segments: accelerated membrane renewal in rods after exposure to light. *Science (Wash. D. C.).* **196:**536–538.
7. Besharse, J. C., J. G. Hollyfield, and M. E. Rayborn. 1977. Turnover of rod photoreceptor outer segments: membrane addition and loss in relationship to light. *J. Cell Biol.* **75:**507–527.
8. Bok, D., and M. O. Hall. 1971. The role of the pigment epithelium in the etiology of inherited retinal dystrophy in the rat. *J. Cell Biol.* **49:**662–682.
9. Bownds, D., A. Gordon-Walker, A. C. Guide-Huguenin, and W. Robinson. 1971. Characterization and analysis of frog photoreceptor membranes. *J. Gen. Physiol.* **58:**225–237.
10. Bridges, C. D. B., J. G. Hollyfield, J. C. Besharse, and M. E. Rayborn. 1976. Visual pigment loss after light-induced shedding of rod outer segments. *Exp. Eye Res.* **23:**637–641.
11. Cohen, A. I. 1968. New evidence supporting the linkage to extracellular space of outer segment saccules of frog cones but not rods. *J. Cell Biol.* **37:**424–444.
12. Coupland, R. E. 1968. Determining sizes and distribution of sizes of spherical bodies such as chromaffin granules in tissue sections. *Nature (Lond.).* **217:**384–388.
13. Currie, J. R., and J. G. Hollyfield. 1977. Darkness is required for shedding in frog rods. Presented at the Association for Research in Vision and Ophthalmology Meeting, Sarasota, Fla., April 1977.
14. Dubin, M. W. 1970. The inner plexiform layer of the vertebrate retina: a quantitative and comparative electron microscopic analysis. *J. Comp. Neurol.* **140:**479–506.
15. Hall, M. O., D. Bok, and A. D. E. Bacharach. 1969. Biosynthesis and assembly of the rod outer segment membrane system: formation and fate of visual pigment in the frog retina. *J. Mol. Biol.* **45:**397–406.
16. Hamburger, V. 1960. A Manual of Experimental Embryology. The University of Chicago Press, Chicago. 221.
17. Hogan, M. J., I. Wood, and R. H. Steinberg. 1974. Phagocytosis by pigment epithelium of human retinal cones. *Nature (Lond.).* **252:**305–307.
18. Hollyfield, J. G., J. C. Besharse, and M. E. Rayborn. 1976. The effect of light on the quantity of phagosomes in the pigment epithelium. *Exp. Eye Res.* **23:**623–635.
19. Ishikawa, T., and E. Yamada. 1970. The degradation of the photoreceptor outer segments within the pigment epithelial cell of rat retina. *J. Electron Microsc.* **19:**85–99.
20. Klein, D. C. 1974. Circadian rhythms in indole metabolism in the rat pineal gland. *In* The Neurosciences Third Study Program. F. O. Schmitt and F. G. Worden, eds. The M. I. T. Press, Cambridge, Mass. 509–515.
21. Kroll, A. J., and R. Machemer. 1968. Experi-

mental retinal detachment in the owl monkey. III. Electronmicroscopy of retina and pigment epithelium. *Am. J. Ophthalmol.* **66:**410-427.

22. LaVail, M. M. 1976. Rod outer segement disc shedding in rat retina: relationship to cyclic lighting. *Science (Wash. D. C.).* **194:**1071-1074.
23. LaVail, M. M. 1976. Rod outer segment disc shedding in relation to cyclic light. *Exp. Eye Res.* **23:**277-280.
24. Sjöstrand, F. S. 1953. The ultrastructure of the outer segments of rods and cones of the eye as revealed by the electron microscope. *J. Cell. Comp. Physiol.* **42:**15-44.
25. Spitznas, M., and M. J. Hogan. 1970. Outer segments of photoreceptors and the retinal pigment epithelium: interrelationships in the human eye. *Arch. Ophthalmol. B. Aires.* **84:**810-819.
26. Taylor, A. C., and J. J. Kollros. 1946. Stages in the normal development of *Rana pipiens* larvae. *Anat. Rec.* **94:**7-23.
27. Young, R. W. 1967. The renewal of photoreceptor outer segments. *J. Cell Biol.* **33:**61-72.
28. Young, R. W. 1968. Passage of newly formed protein through the connecting cilium of retinal rods in the frog. *J. Ultrastruct. Res.* **23:**462-473.
29. Young, R. W., and D. Bok. 1969. Participation of the retinal pigment epithelium in the rod outer segment renewal process. *J. Cell Biol.* **42:**392-403.
30. Young, R. W., and B. Droz. 1968. The renewal of protein in retinal rods and cones. *J. Cell Biol.* **39:**169-184.
31. Young, R. W., and W. T. O'Day. 1977. Rhythmic degradation of outer segment membranes by visual cells in the goldfish. Presented at the Association for Research in Vision and Ophthalmology Meeting, Sarasota, Fla., April 1977.